

## Physical and Genetic Mapping of the *Rhodobacter sphaeroides* 2.4.1 Genome: Presence of Two Unique Circular Chromosomes

ANTONIUS SUWANTO AND SAMUEL KAPLAN†\*

Department of Microbiology, University of Illinois at Urbana-Champaign, Urbana, Illinois 61801

Received 10 April 1989/Accepted 4 August 1989

A macrorestriction map representing the complete physical map of the *Rhodobacter sphaeroides* 2.4.1 chromosomes has been constructed by ordering the chromosomal DNA fragments from total genomic DNA digested with the restriction endonucleases *Ase*I, *Spe*I, *Dra*I, and *Sna*BI. Junction fragments and multiple restriction endonuclease digestions of the chromosomal DNAs derived from wild-type and various mutant strains, in conjunction with Southern hybridization analysis, have been used to order all of the chromosomal DNA fragments. Our results indicate that *R. sphaeroides* 2.4.1 carries two different circular chromosomes of  $3,046 \pm 95$  and  $914 \pm 17$  kilobases (kb). Both chromosome I (3,046 kb) and chromosome II (914 kb) contain rRNA cistrons. It appears that only a single copy of the rRNA genes is contained on chromosome I (*rrnA*) and that two copies are present on chromosome II (*rrnB*, *rrnC*). Additionally, genes for glyceraldehyde 3-phosphate dehydrogenase (*gapB*) and  $\delta$ -aminolevulinic acid synthase (*hemT*) are found on chromosome II. In each instance, there appears to be a second copy of each of these genes on chromosome I, but the extent of the DNA homology is very low. Genes giving rise to enzymes involved in CO<sub>2</sub> fixation and linked to the gene encoding the form I enzyme (i.e., the form I region) are on chromosome I, whereas those genes representing the form II region are on chromosome II. The complete physical and partial genetic maps for each chromosome are presented.

*Rhodobacter sphaeroides* has contributed significantly to our understanding of the molecular genetics of photosynthesis. In addition, many important observations made with this organism have contributed to our understanding at the molecular level of numerous biological and biophysical phenomena, such as photosynthetic membrane biogenesis (25, 26, 34), carbon dioxide fixation (45), the light reactions of photosynthesis (10, 40), pigment biosynthesis (9), and the crystallization of the phototrap (12, 31). To bring these biological and molecular studies to a common biological reference, we have attempted to provide a complete physical and genetic map of this organism. In the accompanying paper, we have demonstrated that the total genome size of this bacterium is about 4,400 kilobases (kb), which comprises the chromosomal DNA ( $3,960 \pm 112$  kb) and the five endogenous plasmid DNAs (approximately 450 kb) (43). A number of genes have been localized to the chromosomal DNA fragments derived from an *Ase*I digest of total genomic DNA, and the location, relative distance, and orientation of certain genes and/or gene clusters have also been established (43). The depth of our understanding of only a handful of procaryotic systems has, with rare exceptions, not been accompanied by an extensive and broad analysis of the total microbial gene pool. We show here that not only is this gene pool varied but also its analysis is likely to be crucial to our exploitation of important biological phenomena.

Genomic mapping can be performed at the level of chromosomal DNA itself (physical mapping) or by following the pattern in which portions of the genome are passed to the progeny (genetic linkage mapping). In bacteria, genetic linkage maps are usually constructed through the use of

plasmids which can mobilize the chromosome over long distances (17, 23). *Escherichia coli*, *Salmonella typhimurium*, *Bacillus subtilis*, and *Pseudomonas aeruginosa* are the bacteria with the most extensive and best studied genetic linkage maps (2, 23, 36, 39).

Physical maps specify the distances between landmarks along a chromosome. Ideally, the distances are measured in base pairs, so that the map provides a direct and accurate description of the chromosomal DNA molecule itself. The most important landmarks in physical mapping (as routinely used in plasmid mapping) are the cleavage sites resulting from the treatment with restriction endonucleases. The enzymes useful for genomic analysis of a particular bacterial genome can be, to a first approximation, predicted from the mole percent G+C of its genomic DNA (35).

The first and largest DNA molecule that has been mapped with rare-cutting restriction enzymes is the single chromosome of *E. coli* (circular, approximately 4,700 kb) (41). Recently, this map has been extended to a higher degree of resolution (Kohara physical map) (30, 44).

In this paper, we describe the strategy used to link the restriction enzyme-generated fragment DNAs derived from the *R. sphaeroides* 2.4.1 chromosomes into two complete physical maps. In addition, we provide compelling evidence for the existence of two unique chromosomes in this bacterium.

### MATERIALS AND METHODS

**Bacterial strains and plasmids.** All bacterial strains, plasmids, and DNA fragments, as well as growth conditions, are described in the accompanying paper (43). To screen for junction fragments we used a cosmid library of *R. sphaeroides* 2.4.1 total genomic DNA. This cosmid library was constructed by S. Dryden and S. Kaplan (unpublished results) by using cosmid vector pLA2917 (1).

\* Corresponding author.

† Present address: Department of Microbiology, University of Texas Medical Center, P.O. Box 20708, F.B. 1.765, Houston, TX 77225.

**Screening for junction fragments from the cosmid library.** The cosmid vector is 21.5 kb long and has two *DraI* restriction endonuclease sites of approximately 0.5 kb flanking the *BglIII* site, the site of insertion of *R. sphaeroides* DNA (*DraI-BglIII-DraI*). Since the cosmid vector does not possess an *AseI* site, we screened for cosmids containing an *AseI* site(s) in their insert DNA (*R. sphaeroides* 2.4.1) as follows. Cosmid DNA was isolated by the alkaline lysis method (7) and digested with *DraI* and *DraI-AseI* in a double digest, and the restriction endonuclease digests were electrophoresed side by side by nonpulsed horizontal gel electrophoresis (0.7% [wt/vol] gel). If the insert DNA contains an *AseI* site, the *DraI-AseI* double digest will generate more DNA fragments than the single *DraI* digestion will. We chose *DraI* as a secondary enzyme to detect the *AseI* sites because *DraI* is also a rare cutter for *R. sphaeroides* 2.4.1 DNA, yielding only a small number of DNA fragments, whose pattern can be easily compared with that obtained from the *DraI-AseI* double digestion. The *R. sphaeroides* 2.4.1 DNA fragments containing an *AseI* site(s) were designated *AseI* junction fragments (42); they were ultimately used as probes of the *AseI*-digested total genomic DNA to determine which DNA fragments are adjacent to one another.

**Isolation of the 214-kb *AseI*-generated fragment DNAs for restriction digest analysis.** We electrophoresed an *AseI* digest of total genomic DNA in two lanes of a transverse alternating field electrophoresis (TAFE) gel (0.75% SeaKem GTG agarose [FMC Corp.]; stage 2: 23-s pulse for 18 h). After electrophoresis, but before staining with ethidium bromide, we removed one lane of the agarose gel and saved it at 4°C while we stained the other lane with ethidium bromide. Having located the 214-kb *AseI* DNA fragment from the ethidium bromide-stained gel, we then excised the 214-kb fragment from the gel slice. The excised gel fragment was placed in 1× TE (10 mM Tris hydrochloride, 1 mM EDTA [pH 8.0]) at 4°C, held overnight, and processed for digestion as described in the accompanying paper (43). The 214-kb DNA fragment was digested with 30 U of *EcoRI* for 5 h. In addition, we loaded λ DNA, treated identically to the 214-kb *AseI* fragment used as a control to monitor the completeness of the *EcoRI* digestion, into the other lanes of the same gel.

The separation and isolation of DNA fragments, as well as all other molecular biological techniques, are described in the accompanying paper (43).

**Materials.** Complete details of the materials used are given in the accompanying paper (43).

## RESULTS

**Junction fragment analysis.** We screened 350 cosmids for the presence of *AseI* junction fragments from a total of 800 cosmids in the pLA2917 cosmid library. We identified six cosmids containing *AseI* restriction endonuclease sites; however, only two of these (cos662 and cos440) gave true junction fragment signals following Southern hybridization analysis. The DNA inserts from the other cosmids hybridized to more than two bands in the *AseI* digest of total genomic DNA. Two of these four cosmid-identified DNA fragments were derived from the endogenous plasmids. We did not characterize these four *AseI*-containing cosmids further.

The DNA from cos662, which contains a junction fragment, hybridized only to two unique *AseI*-generated fragments (244- and 18-kb fragments) (Fig. 1A, lane 2). To determine whether this is a "true" junction fragment or only

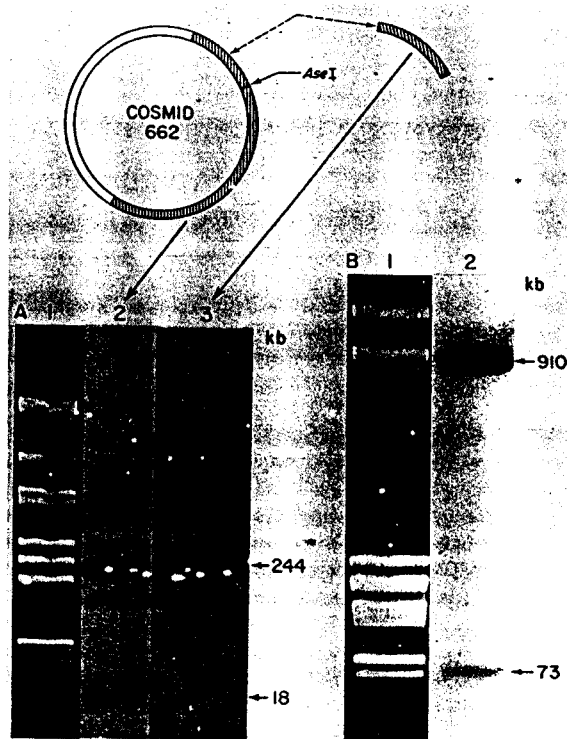


FIG. 1. Junction fragment analysis. (A) The *R. sphaeroides* 2.4.1 DNA fragment from cos662 is a junction fragment joining the 244- and 18-kb *AseI* fragments. Lanes: 1, ethidium bromide-stained gel of *AseI* digest of total genomic DNA (TAFE run with a 23-s pulse for 16 h); 2, autoradiogram of lane 1 with whole cos662 DNA as a probe; 3, autoradiogram as in lane 2 with a small portion of *R. sphaeroides* insert DNA from cos662 as a probe. (B) *R. sphaeroides* 2.4.1 DNA fragment present in cos440 is a junction fragment between the 73- and 910-kb *AseI* fragments. Lanes: 1, EtBr-stained gel (TAFE run with a 55-s pulse for 18 h); 2, autoradiogram of lane 1 with whole cos440 as a probe.

an artifact derived from a repetitive DNA sequence (should such be present in *R. sphaeroides*), we isolated a subclone of the insert DNA from cos662 and used that as a probe of the *AseI* digest of total genomic DNA. This subclone of cos662 hybridized only to the 244-kb *AseI* fragment (Fig. 1A, lane 3). This result unambiguously demonstrated that cos662 contains a true junction fragment which links the 18- and 244-kb *AseI* fragments. The linkage between the 18- and 244-kb *AseI* fragments was additionally confirmed by using *SpeI* and *DraI* as described below. Figure 1B demonstrates the existence of a second junction fragment (cos440), which linked the 73- and 910-kb *AseI* fragments.

Previous experiments indicated that the 18- and 73-kb *AseI* fragments are linked and that these two fragments contain many of the genes associated with the photosynthetic spectral complexes (43). Therefore, we were able to show that the four *AseI* fragments are linked to each other in the order 244, 18, 73, and 910 kb, or G-J-I-B (43).

Two other *AseI* fragments, which were also linked by using a junction fragment analysis, are the 214- and 340-kb *AseI* fragments. When we used the 5.8-kb *EcoRI* fragment (fragment a), which contains a single *AseI* site as a probe of the *AseI* digest of total genomic DNA, we saw a hybridization signal with three of the DNA fragments instead of just two of the fragments, we would normally be expected for a

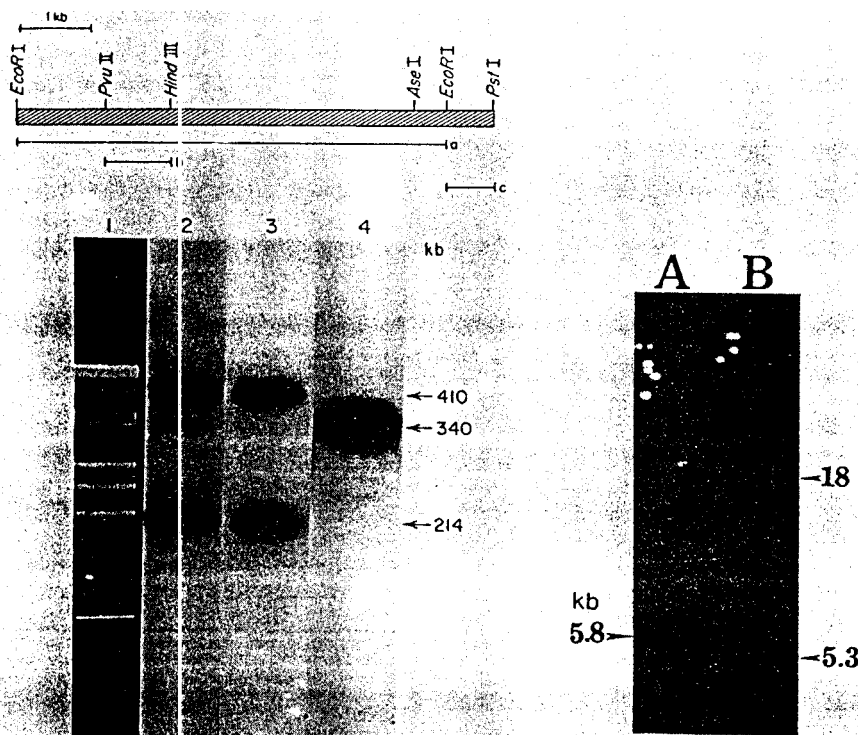


FIG. 2. Joining of the 340- and 214-kb *AseI* fragments. Lanes: 1, EtBr-stained gel (TAFE run with a 16-s pulse for 17 h); 2, autoradiogram of lane 1 with an *EcoRI-EcoRI* fragment (fragment a) as a probe; 3, autoradiogram as in lane 2 with a *PvuII-HindIII* fragment (fragment b) as a probe; 4, autoradiogram as in lane 2 with an *EcoRI-PstI* fragment (fragment c) as a probe; A, autoradiogram of *EcoRI*-digested total genomic DNA probed with fragment a; B, autoradiogram of *EcoRI*-digested 214-kb *AseI* fragment probed with fragment a.

true junction fragment (Fig. 2, lane 2). The sizes of these *AseI* fragments are 410, 340, and 214 kb. To confirm which of the DNA fragments were, in fact, the true neighboring fragments, we isolated the upstream (*PvuII-HindIII*; fragment b) and the downstream (*EcoRI-PstI*; fragment c) DNA fragments relative to the *AseI* site (Fig. 2). Fragment b (upstream) hybridized only to the 410- and 214-kb *AseI* fragments, and fragment c (downstream) hybridized only to the 340-kb *AseI* fragment (Fig. 2, lanes 3 and 4, respectively). These results clearly demonstrated that the true junction fragment should lie between either the 340- and 214-kb fragments or the 340- and 410-kb fragments, but not between the 214- and 410-kb fragments.

Therefore, it became imperative to distinguish which of the 214- or 410-kb fragments were linked to the 340-kb fragment. This was accomplished as follows. The 5.8-kb *EcoRI* fragment was isolated (Dryden and Kaplan, unpublished) from one of three unique hybridization signals (these correspond to the rRNA cistrons) from an *EcoRI* digest of total genomic DNA. Second, we isolated the 214-kb *AseI* fragment and digested it with *EcoRI* as described in Materials and Methods. The digest was electrophoresed in a nonpulsed 1% agarose gel side by side with *EcoRI*-digested total genomic DNA. Southern hybridization analysis, using the 5.8-kb *EcoRI* fragment (Fig. 2, fragment a) as a probe of these *EcoRI* digests, is shown in Fig. 2, lanes A and B. There were two unique *EcoRI* signals residing on the 214-kb *AseI* fragment (Fig. 2, lane B), and one of these is the 5.8-kb *EcoRI* fragment, which was approximately 500 base pairs smaller than the corresponding 5.8-kb *EcoRI* fragment (fragment a) observed in the digest of total genomic DNA (Fig. 2, lane A). This 5.8-kb *EcoRI* fragment, which is derived from the 214-kb *AseI* fragment, should be approximately 500 base

pairs smaller than fragment a because an *AseI* site is located approximately 500 base pairs upstream of the *EcoRI* restriction site located at the right end of fragment a (see the restriction map in Fig. 2). Thus, we were able to conclude that the 214- and 340-kb *AseI* fragments are linked and that the 214-kb *AseI* fragment should contain two of the three unique *EcoRI* signals (*rrnB* and *rrnC* operons) observed in the *EcoRI* digest of total genomic DNA (Dryden and Kaplan, unpublished).

The relative orientation of the 214- and 340-kb *AseI* fragments was determined. In a PRKB<sup>-</sup> strain (43), the 340-kb *AseI* fragment could be digested into 280- and 60-kb *AseI* fragments because of the presence of a spectinomycin-streptomycin resistance cartridge in this fragment (43; see Fig. 7C). Southern hybridization analysis was performed by using the *EcoRI-PstI* fragment (Fig. 2, fragment c) as a probe of the *AseI*-digested total genomic DNA derived from the PRKB<sup>-</sup> strain. The results indicated that fragment c was located in the 280-kb *AseI* fragment (data not shown), which means that the junction between the 214- and 340-kb *AseI* fragment is located 280 kb upstream of *prkB* (43; see Fig. 7C).

**Joining of the 910- and 410-kb *AseI* fragments.** *SpeI*-digested total genomic DNA revealed a single large (1,645-kb) *SpeI* fragment (43). Southern hybridization analysis of *SpeI*-digested total genomic DNA with *pufBA*, *nifHDK*, and *cos662* (244- and 18-kb *AseI* junction fragment) as probes showed that all of these DNA fragments were located within the 1,645-kb *SpeI* fragment. An *SpeI-AseI* double digestion of total genomic DNA revealed that the 244-, 18-, 73-, and 910-kb fragments corresponded precisely to the identical DNA fragments observed for an *AseI* digest of total genomic DNA (data not shown) and, hence, that these four fragments

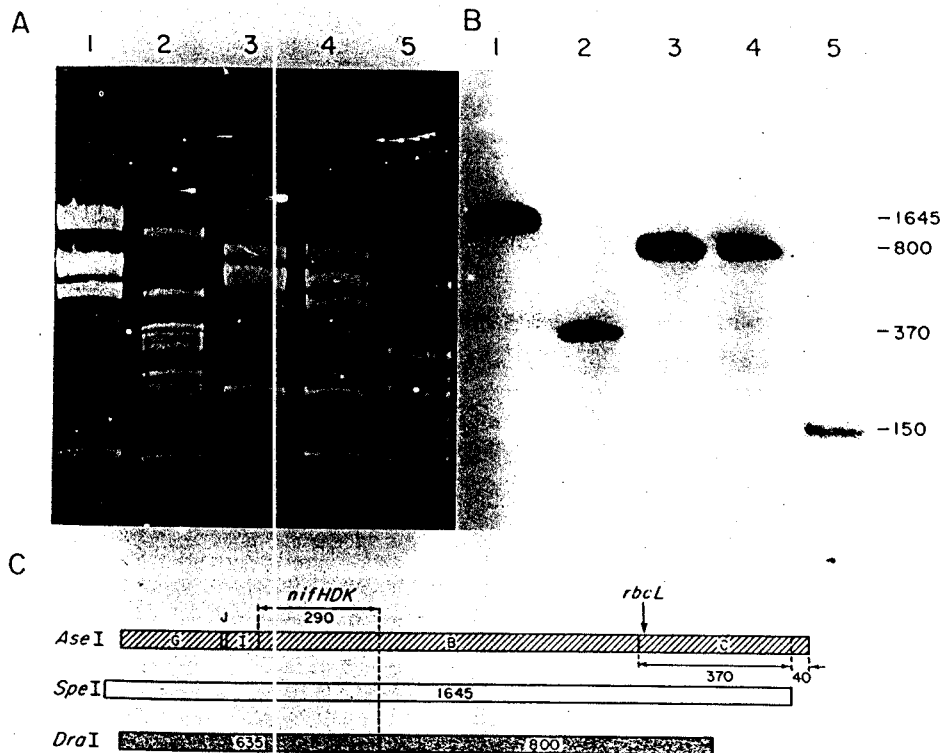


FIG. 3. Joining of the 910- and 410-kb *AseI* fragments. (A) Ethidium bromide-stained gel of 2.4.1 total genomic DNA digested with *SpeI* (lane 1), *SpeI-AseI* (lane 2), *DraI* (lane 3), *SpeI-DraI* (lane 4), or *DraI-AseI* (lane 5). TAFE was run with a 45-s pulse for 9 h (stage 2), a 23-s pulse for 7 h (stage 3), and a 7-s pulse for 8 h (stage 4). (B) Autoradiogram of panel A with *rbcL* as a probe. (C) Schematic representation of the data.

must not contain an *SpeI* restriction site. Therefore, we were able to directly demonstrate that the 244-, 18-, 73-, and 910-kb *AseI* fragments must reside within the large (1,645-kb) *SpeI* fragment. In addition, these data also directly confirmed the validity of the junction fragment analysis described previously which linked the 244-, 18-, 73-, and 910-kb *AseI* fragments.

Furthermore, Southern hybridization analysis indicated that *rbcL* was also located on the 1,645-kb *SpeI* fragment (Fig. 3A and B, lanes 1). Since *rbcL* is a unique marker for the 410-kb *AseI* fragment (43; see Fig. 4), the 410-kb *AseI* fragment must be located at one end of the 1,645-kb *SpeI* fragment, i.e., linked to either the 910- or 244-kb *AseI* fragment. Figure 3A and B, lanes 2, show that *rbcL* can be assigned to a 370-kb *SpeI-AseI* fragment, which unambiguously reveals that one end of the 1,645-kb *SpeI* fragment contains the 370-kb *AseI-SpeI* fragment derived from the 410-kb *AseI* fragment, which, in turn, contains the *rbcL* gene. To determine whether the 410-kb *AseI* fragment is linked to either the 244- or the 910-kb *AseI* fragment, we performed the following experiments. *rbcL* was used to probe the *DraI*, *DraI-SpeI*, and *DraI-AseI* digests of total genomic DNA (Fig. 3A, lanes 3 to 5). Hybridization signals were observed to the 800-kb *DraI* and *DraI-SpeI* fragments (Fig. 3B, lanes 3 and 4) as well as to the 150-kb *DraI-AseI* fragment (Fig. 3B, lane 5). Other results (data not shown) indicated that the 635-kb *DraI* fragment encompasses the 244-, 18-, and 73-kb (G, J, and I, respectively) *AseI* fragments as well as a 290-kb portion of the 910-kb *AseI* fragment. The electrophoretic banding pattern revealed that the 635-kb *DraI* fragment remained intact following double digestion of total genomic DNA with *DraI-SpeI* (data not

shown). Thus, the 635-kb *DraI* fragment must lie within the 1,645-kb *SpeI* fragment and should carry *nifHDK* and *pufBA* (43). In addition, the 800-kb *DraI* fragment also remained intact following *DraI-SpeI* double digestion (Fig. 3A, lane 4). Therefore, the 800-kb *DraI* fragment must also lie within the 1,645-kb *SpeI* fragment and hence contains *rbcL* (Fig. 3B, lanes 3 and 4). Interpretation of these results are simplified in Fig. 3C. Notice the positions of *AseI*, *DraI*, and *SpeI*. Taking these data together, we were able to demonstrate that the 410-kb *AseI* fragment (fragment C) is linked to the 910-kb *AseI* fragment (fragment B) with the orientation shown in Fig. 3C.

Intermediate physical map and the position of the two largest *SnaBI* fragments. Using similar approaches to those described above for the joining of the 410- and 910-kb *AseI* fragments, as well as comparison of the electrophoretic banding patterns of several mutant strains with that of the wild-type strain, we were able to order all of the *AseI*-generated chromosomal fragments into two linear linkage groups, i.e., D-E-H and G-J-I-B-C-F-A-K. Assuming that the chromosome of *R. sphaeroides* is circular, the position of D-E-H would have to be between G and K, as shown in the intermediate physical map in Fig. 4, with the relative orientation being either D-E-H or H-E-D relative to G and K.

*SpeI* digested the two largest *SnaBI* fragments (1,225 and 1200 kb) into 900-kb, 800-kb, and smaller *SnaBI-SpeI* fragments. The 900- and 800-kb *SnaBI-SpeI* fragments must be derived from the 1,225- and the 1,200-kb *SnaBI* fragments. The only *SpeI* fragment which is large enough to yield both a 900- and an 800-kb *SnaBI-SpeI* fragment is the largest (1,645-kb) *SpeI* fragment, since the second-largest *SpeI* fragment is only 735 kb. This means that there is a single

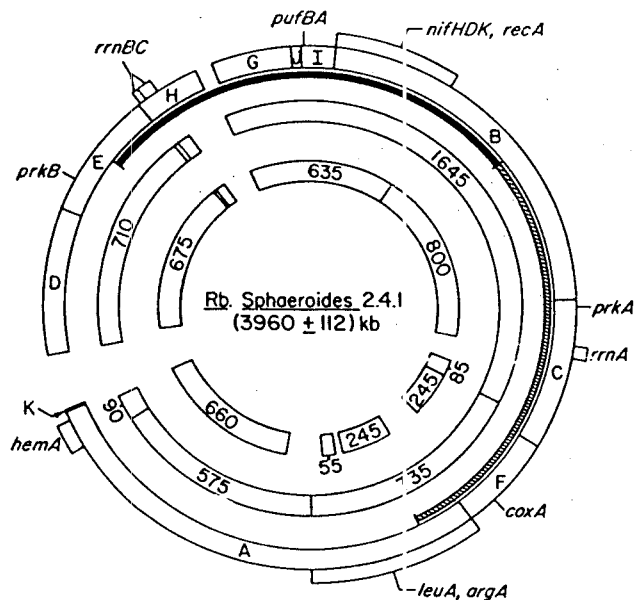


FIG. 4. Intermediate physical map of *R. sphaeroides* chromosomes to show the only possible location of the D-E-H *AseI* fragments relative to the other *AseI* chromosomal fragments. The outer circle represents the *AseI* map, the middle circle represents the *SpeI* map, and the inner circle is for the *DraI* map. The thickened line between the *AseI* and *SpeI* restriction maps represents the position of the two largest *SnaBI* fragments.

*SnaBI* site approximately in the middle of the 1,645-kb *SpeI* fragment, so that each of the two largest *SnaBI* fragments extends beyond the ends of the 1,645-kb *SpeI* fragment, ultimately yielding the 900- and 800-kb *SnaBI-SpeI* fragments (Fig. 4). Therefore, by using a specific probe, we can easily determine which of the two largest *SnaBI* fragments gives rise to each of the 900- and 800-kb *SnaBI-SpeI* fragments. When *nifHDK* was used as a probe, it hybridized only to the 900-kb *SnaBI-SpeI* fragment, whereas when used as a probe, *rbcL* hybridized uniquely to the 800-kb *SnaBI-SpeI* fragment as well as to the 1,200-kb *SnaBI* fragment (*coxA* hybridized to the 1,200-kb *SnaBI* fragment). Thus, *coxA* must lie within the 1,200-kb *SnaBI* fragment, which also encompasses *rbcL*, yielding the 800- and 400-kb *SnaBI-SpeI* fragments upon double digestion (Fig. 4). Therefore, we were able to assign the 1,200-kb *SnaBI* fragment, which carries the *rbcL* and *coxA* markers, to the position shown in Fig. 4. The 900-kb *SnaBI-SpeI* fragment encoding *nifHDK* must be derived from the 1,225-kb *SnaBI* fragment which includes *nifHDK* as well as the *AseI* fragments designated I, J, and G (Fig. 4).

The validity of the assignment of the locations of these largest *SnaBI* fragments was confirmed by *SnaBI-DraI* and *SnaBI-AseI* double digestions in conjunction with Southern hybridization analysis with specific probes assigned to each fragment (data not shown). Thus, we were able to assign and locate unambiguously the two largest *SnaBI* fragments shown in Fig. 4.

**Are there two chromosomes?** As described above, the largest *SnaBI* fragment (1,225 kb) extended into approximately half of *AseI* fragment B and included in its entirety *AseI* fragments I, J, and G (Fig. 4). The size of the *SnaBI-SpeI* fragment covering these same *AseI* fragments is approximately 900 kb. Thus, if linkage group D-E-H is joined to the larger linkage group, the other end of the 1,225-kb

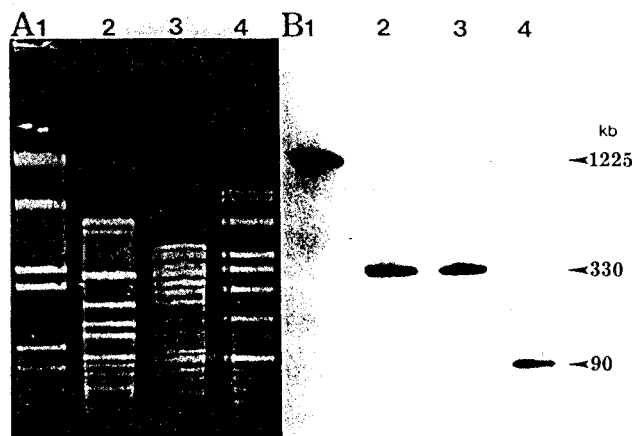


FIG. 5. The evidence that the *AseI* fragments D-E-H are separate from fragments G-J-I-B-C-F-A-K, leading to two circular chromosomes in *R. sphaeroides*. (A) Ethidium bromide-stained gel of 2.4.1 total genomic DNA digested with *SnaBI* (lane 1), *SnaBI-DraI* (lane 2), *SnaBI-AseI* (lane 3); or *SnaBI-SpeI* (lane 4). TAFE was run with a 50-s pulse for 9 h (stage 2), a 23-s pulse for 7 h (stage 3), and an 8-s pulse for 4 h (stage 4). (B) Autoradiogram of panel A with *hemA* as a probe.

*SnaBI* fragment should be located somewhere in *AseI* fragment D or E, so that the total *SnaBI-SnaBI* fragment length of 1,225 kb was accommodated (Fig. 4). Hybridization analysis indicated that the 784-kb *SnaBI* fragment resides in its entirety within the three contiguous *AseI* fragments D-E-H, whose total size is approximately 914 kb. This means that approximately 130 kb of DNA is unaccounted for (914 kb less 784 kb) and, accordingly, that this 130-kb fragment must be part of the large (1,225-kb) *SnaBI* fragment. Arithmetically, however, this is impossible, since the 900-kb *SnaBI-SpeI* fragment must, at the very least, neighbor a 300-kb DNA fragment to provide a total *SnaBI* fragment length of 1,225 kb. This requirement cannot be met with a 130-kb DNA fragment. This was the first substantial evidence that the three *AseI* fragments, D, E, and H, could not be joined to the other contiguous set of *AseI* fragments. Hybridization analysis with *hemA* as a probe (Fig. 5) was able to resolve this paradox.

**The circularity of chromosome I.** Southern hybridization analysis in Fig. 5, lanes 1, shows that *hemA* was located on the largest (1,225-kb) *SnaBI* fragment, which means that fragment G must be linked to fragment K (Fig. 4). This conclusion was further confirmed by a hybridization analysis involving a series of double digestions with *SnaBI-DraI*-, *SnaBI-AseI*-, and *SnaBI-SpeI*-, as well as *SnaBI-SpeI*-digested total genomic DNA from strain Ga. *hemA* is located on the 330-kb *SnaBI-DraI* fragment and the 330-kb *SnaBI-AseI* fragment (Fig. 5, lanes 2 and 3), as would be anticipated if fragment G were joined to fragment K (Fig. 4); *hemA* also resides on the 90-kb *SnaBI-SpeI*-generated fragment (Fig. 5, lane 4), which is consistent with the previous experiments that *hemA* has also been located on the 90-kb *SpeI* fragment, which has been shown to reside entirely within fragment A (data not shown). Thus, we were forced to conclude that the three contiguous *AseI* fragments D-E-H were physically separated from the second set of contiguous *AseI* fragments, and at the same time, we demonstrated that the contiguous fragments G-J-I-B-C-F-A-K were circular, with a total size of  $3,046 \pm 95$  kb. The G-J-I-B-C-F-A-K fragments have been designated chromosome I, and the D-E-H fragments ( $914 \pm$

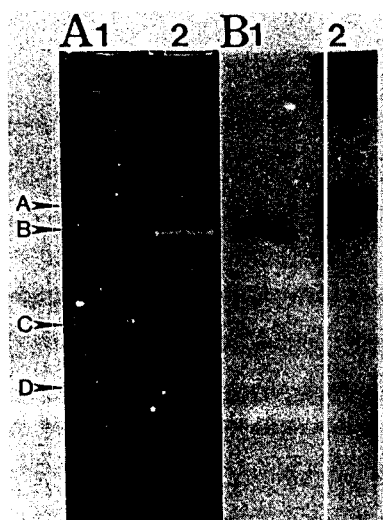


FIG. 6. Southern hybridization analysis of electrophoresed undigested total genomic DNA. (A) Ethidium bromide-stained gel. TAFE was run with a 50-s pulse for 21 h. Lane: 1, strain MS2 II-6; 2, strain MS2-R. (B) Autoradiogram of panel A with Tn5 as a probe.

17 kb) have been designated chromosome II, for the reasons that are explained below.

**The existence of chromosome II.** There is additional evidence which supports the presence of two chromosomes in *R. sphaeroides* 2.4.1. Total undigested genomic DNA from strains MS2 II-6 (*pigA*) and MS2-R (*Arg<sup>-</sup>*) (43) were electrophoresed side by side (Fig. 6A). Under these conditions, we were able to observe the conventional supercoiled endogenous plasmid regions designated C and D, the sharply banded linearized form of chromosome II designated region B, and the broad band of DNA fragments derived from chromosome I, indicated as region A. In this case (Fig. 6), strain MS2 II-6 yielded a very small amount of linearized chromosomes I and II (Fig. 6A, lane 1) compared with that observed for strain MS2-R (Fig. 6A, lane 2). Southern hybridization with Tn5 as a probe showed that Tn5 hybridized only to chromosome II derived from strain MS2 II-6 and only to chromosome I derived from strain MS2-R (Fig. 6B, lanes 1 and 2, respectively). These results were not unexpected, since strain MS2 II-6 contains Tn5 in *AseI* fragment D (i.e., in chromosome II), whereas strain MS2-R contains Tn5 in *AseI* fragment A (i.e., in chromosome I) (43) (Fig. 4). The experiments reported here clearly show that chromosome II is not a concatemeric form of any of the endogenous plasmids; i.e., it is a unique physical entity, since if it were a concatemeric form of one or more of the endogenous plasmids, the hybridization signal seen in Fig. 6B, lane 1, would have been observed in the region of the endogenous plasmids in addition to region B.

It is possible that chromosome II and chromosome I can form a cointegrate structure yielding one fused chromosome, and in this case, we would expect to see cross-hybridization to region A as well as region B in Fig. 6. However, our results show that there was no observable cross-hybridization signal to region A (Fig. 6B, lane 1). This is also true for the hybridization signal in region A, cross-hybridizing with region B (Fig. 6B, lane 2). It is also conceivable that the supercoiled form of chromosome II migrates in a TAFE gel, although this does not appear likely. However, we must postulate that the DNA fragment seen in region B (Fig. 6A) is the linear form of chromosome II, on the basis of the

following observations. The TAFE gel analysis as performed in Fig. 6A showed that when DNA was derived from log-phase cells, region B as well as region A was almost undetectable and became progressively visible as the age of the culture increased, well into the stationary phase (data not shown). We would expect these conditions to lead to the accumulation of double-strand DNA breaks, since nicked circular DNA from such large molecules will not migrate under the conditions used here. Topoisomerase I treatment (43) showed that regions C and D were sensitive to relaxation, whereas regions B and A remained unaffected; moreover, movement of regions B and A was pulse time dependent (data not shown). Although we designated region A as a linear form of chromosome I, for the same reasons as described for chromosome II we cannot exclude the possibility of the existence of supercoiled DNA, since both topoisomerase I and pulse-time experiments may not work as expected for such a large DNA molecule (18).

Hybridization analysis of total undigested DNA electrophoresed as described for Fig. 6 with several different probes (*puhA*, *nifHDK*, *fbc*, *rrn*, *hemT*, and *hemA*) indicated that only *rrn* and *hemT* hybridized to chromosome II (data not shown). These markers reside on *AseI* fragments H and E, respectively (43) (Fig. 4). Furthermore, in the PRKB<sup>-</sup> strain (43), a probe composed of the spectinomycin-streptomycin resistance cartridge also hybridized only to chromosome II (data not shown). Finally, using a long pulse period (50 to 60 s), we were able to resolve the DNA fragments corresponding to either chromosome I or chromosome II (Fig. 6A, lane 2). These results, as well as those presented below, underline our reasoning for the existence of two unique chromosomal DNA species in *R. sphaeroides* 2.4.1.

**The circularity of chromosome II.** We conducted a series of experiments to determine whether chromosome II is circular. A gel insert containing undigested total genomic DNA was electrophoresed with a 50-s pulse for 18 h, and then the insert was removed from the well, digested with *AseI*, and electrophoresed a second time side by side with an *AseI* digest of total genomic DNA which had not previously been subjected to electrophoresis. Ethidium bromide staining of each sample revealed that the band intensity of each corresponding *AseI* fragment prior to digestion was similar to the sample which had not been electrophoresed prior to digestion (Fig. 7). If chromosome II were linear, it should have completely traveled the gel during the initial electrophoretic period conducted prior to digestion with *AseI*, and therefore we should not have observed the 360-, 340-, and 214-kb *AseI* fragments, i.e., fragments D, E, and H, respectively, making up chromosome II. The fact that we observed similar band intensities when comparing the 360-, 340-, and 214-kb *AseI* fragments derived from each of the gel inserts indicated that only a small portion of chromosome II was linearized during the initial processing of the gel insert and therefore that most of the population of chromosome II was in either the open-circular or relaxed form, which initially failed to migrate into the gel during the conditions of preelectrophoresis (this must also be true for chromosome I). Therefore, following digestion with *AseI*, the DNA fragments making up chromosome II which were present in each gel insert were resolved in a similar fashion and in similar amounts.

The circularity of chromosome II was also directly supported by the following experiments. Southern hybridization data revealed that *pigB* was located on the 214-kb *AseI* fragment (fragment H) as well as on a 130-kb *SnaBI* fragment (data not shown). Further analysis with *SpeI* and *DraI* facilitated the unambiguous location of the 130-kb *SnaBI*

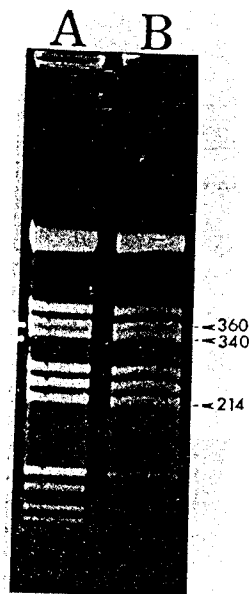


FIG. 7. Comparison of *AseI* fragments generated by an *AseI* digest of total genomic DNA with or without electrophoretic treatment before digestion of the gel insert. TAFE was run with a 23-s pulse for 18 h. (A) Without preelectrophoresis. (B) With preelectrophoresis.

fragment relative to the other restriction enzyme fragments such that the 130-kb *SnaBI* fragment behaves as a junction fragment between *AseI* fragments H and D, which would close the contiguous H-E-D into a circle. Proof that the 130-kb *SnaBI* fragment is a junction fragment between H and D was confirmed as follows. The 130-kb *SnaBI* fragment was isolated from low-melting-point agarose and used as a probe of the *AseI*-digested total genomic DNA. The results show that the 130-kb *SnaBI* probe hybridized to both the 214- and 360-kb *AseI* fragments, indicating that the 130-kb *SnaBI* fragment is a true junction fragment between *AseI* fragments H and D, thereby further substantiating our conclusion that fragments H-E-D are physically formed into a circle (data not shown).

Together, these results allowed us to demonstrate the existence of two unique circular chromosomes in *R. sphaeroides* 2.4.1. Additionally, we have been able to construct the complete macrorestriction maps for the *AseI*, *SpeI*, and *SnaBI* fragments corresponding to each of these two chromosomes (Fig. 8), as well as a limited genetic map of the genome of this bacterium.

#### DISCUSSION

Screening for junction fragments containing specific rare restriction sites is basically simple and should be facilitated by the construction of a library that is easily screened for the presence of the restriction enzyme sites in question (37). In addition, a true junction fragment will clearly designate the two DNA fragments which should be linked to one another, as has been described here. However, not every potential junction fragment yields a satisfactory result, although the DNA fragment contains the restriction enzyme site of interest. Occasionally, as described here, we find a junction fragment which gives more than two hybridization signals (Fig. 2). For the junction fragment shown in Fig. 2, whose DNA length has now been accurately mapped, we were able

to resolve the problem by using several of the strategies described above, such as using only a certain portion of the DNA from the original fragment as a probe. However, a resolution of the apparent ambiguity would be more laborious if the junction fragment had not been fully characterized. A second limitation of this approach is that the library tends to have certain junction fragments as a higher proportion of the theoretical total than might be anticipated, so that we obtained the same junction fragment more than once during the screening process. Such apparent nonrandomness has many underlying causes, and had we screened a second or third independent library, we would most probably have found most of the potential junction fragments we sought. Nonetheless, four such fragments were used during these studies.

Overlapping and double-digestion restriction enzyme analysis, in conjunction with Southern hybridizations with specific and well-characterized probes, was used to complete the entire physical maps of the two *R. sphaeroides* chromosomes. Restriction enzyme analysis also provided the additional advantage of being able to narrow the location of certain genes. Finally, restriction enzyme analysis served as an independent approach used to judge both the validity of the junction fragment analysis and the physical linkage ultimately constructed by the use of restriction enzymes themselves.

Several strains of gram-negative bacteria such as *Rhizobium*, *Agrobacterium*, *Alcaligenes*, *Pseudomonas*, and *Paracoccus* spp. harbor high-molecular-size plasmids of sizes ranging from 400 to approximately 1,500 kb (3, 19, 22). *Rhizobium meliloti* carries two megaplasmids (pSym) of approximately 1,500 kb each (3), and these plasmids have been extensively studied for their role(s) in symbiotic nitrogen fixation and nodulation (4, 21, 24). *Agrobacterium tumefaciens* C58 carries two endogenous plasmids, one being the 200-kb Ti plasmid that is responsible for crown gall tumor formation, and the other being a larger cryptic plasmid, pAtC58 (22, 46). In *Alcaligenes eutrophus* H16, the megaplasmid pHG1 (450 kb) was found to encode both the structural and the regulatory genes for the hydrogenase (14, 15, 20, 32). This organism also contains two sets each of ribulose biphosphate carboxylase (*rbcL*, *S*) and phosphoribulokinase (*prk*) genes; one set is in the chromosome and the other is in the megaplasmid (8, 29). *Paracoccus denitrificans* harbors a cryptic megaplasmid larger than 700 kb (19), whereas some *Pseudomonas* plasmids encode enzymes for aromatic degradation (13) as well as the biosynthesis of a plant phytotoxin (6). Thus, the existence of very large extrachromosomal DNA is widespread among these and, doubtless, numerous other bacteria.

From the standpoint of DNA size, chromosome II of *R. sphaeroides* 2.4.1 may be considered a somewhat large, extrachromosomal DNA element, as described above. However, the fact that chromosome II carries rRNA cistrons (*rnnB* and *rnnC*) (Dryden and Kaplan, unpublished) as well as the gene for glyceraldehyde-3-phosphate dehydrogenase (*gapB*) makes this *R. sphaeroides* 2.4.1 chromosome extraordinary. The larger chromosome, chromosome I, appears to contain only a single rRNA cistron (Dryden and Kaplan, unpublished). As far as we know, *rnn* and *gap* are only found in the "chromosome" of procaryotic organisms and are considered to be essential for normal growth. On the basis of the distribution of *rnn* cistrons in *R. sphaeroides* (a total of three [Dryden and Kaplan, unpublished]), we feel obligated to designate the 914-kb DNA molecule a chromosome rather than a plasmid. It is also interesting that the

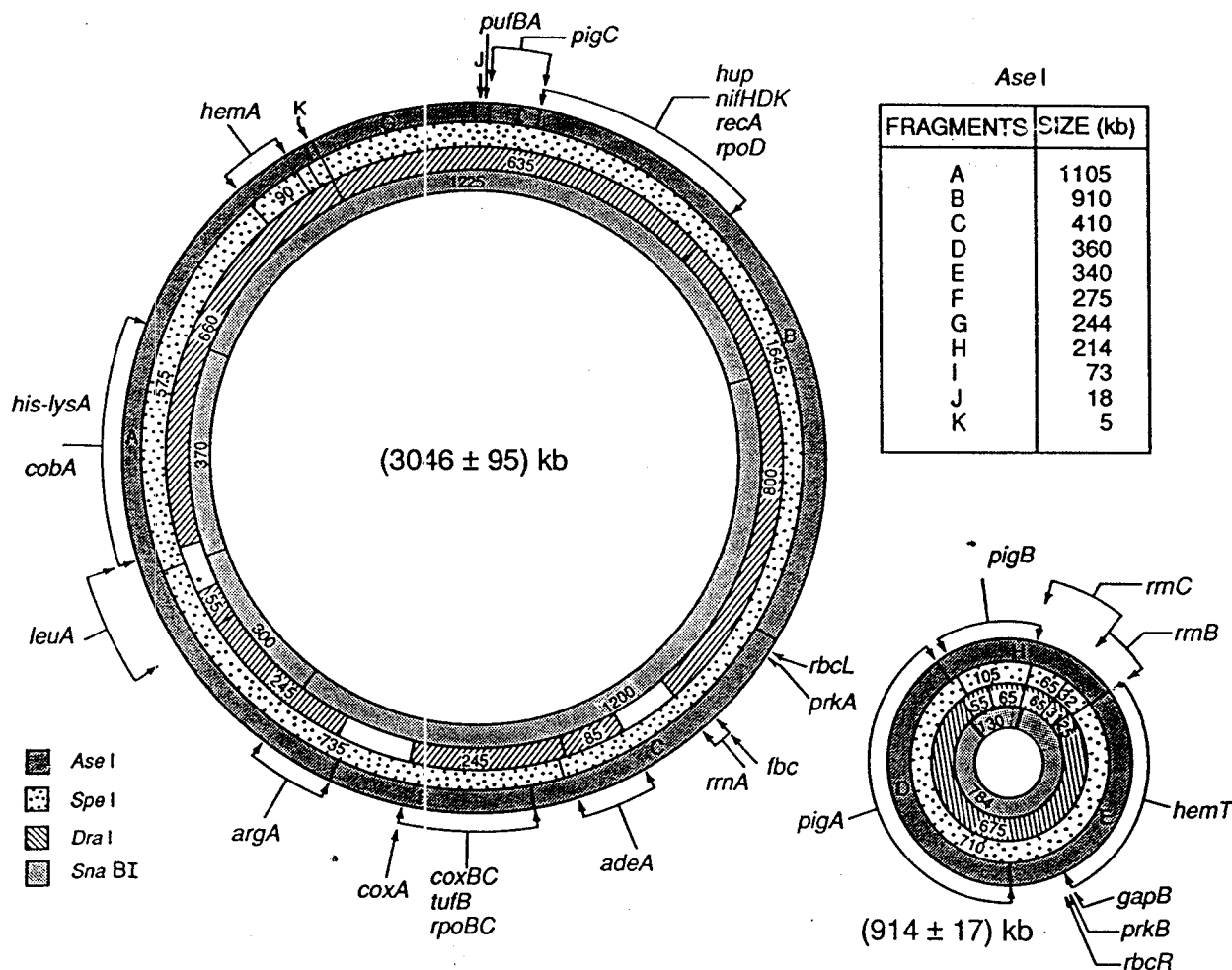


FIG. 8. The entire physical and limited genetic maps of the two *R. sphaeroides* chromosomes. The number of *Spe*I, *Dra*I, and *Sna*BI fragments and the lengths of each fragment (in kilobases) are indicated. The asterisk near the 55-kb *Dra*I fragment indicates that the location of this fragment is somewhere between the 660- and 245-kb *Dra*I fragments but must be inside the 735-kb *Spe*I fragment.

*nifHDK* genes reside on chromosome I in *R. sphaeroides*, whereas they are on the megaplasmid in *Rizobium meliloti*; furthermore, as in *Alcaligenes eutrophus*, *R. sphaeroides* carries one set of genes for carbon dioxide fixation in chromosome I and the other set in chromosome II. However, unlike *Alcaligenes eutrophus*, the two forms of ribulose biphosphate carboxylase in *R. sphaeroides* are different (*rbcL<sub>S</sub>* versus *rbcR*) (16).

We originally questioned whether chromosome II was circular or linear, since a large linear plasmid (approximately 520 kb), designated the giant linear plasmid, has been described for several *Streptomyces* strains (27, 28). However, we have proven here that both of the *Rb. sphaeroides* 2.4.1 chromosomes are circular.

The banding intensity of the ethidium bromide-stained gel indicated that *Ase*I fragments D, E, and H were of equal intensity to essentially all of the other *Ase*I fragments derived from chromosome I, and this was also true for the DNA fragments generated by using the other restriction enzymes. On the basis of this observation, we must infer that chromosomes I and II are present in a 1:1 ratio.

Furthermore, we have directly demonstrated, by using probes specific for either chromosome I or chromosome II, that these do not normally exist as a cointegrate structure in an exponential culture of *R. sphaeroides* under aerobic or

photoheterotrophic conditions. Whether these two chromosomes may transiently exist as a single chromosome is unknown at present. However, such an existence cannot be the normal state over much of the life cycle of *R. sphaeroides*.

The genomic organization of *R. sphaeroides* 2.4.1 presented here is one of the few complete bacterial restriction maps constructed mainly by physical methods (5, 11, 30, 33, 38) and the second to be determined entirely by Southern hybridization analysis of fragments separated by pulsed-field gel electrophoresis (33). However, the results presented here provide the first representation of a more complex overall genomic architecture than for the other bacteria which have been physically mapped. *R. sphaeroides* 2.4.1 carries two different chromosomes and five endogenous plasmids, giving a total of seven replicons and a total genome size of about 4,400 kb. In addition, more than 30 genetic markers have been localized to the physical map of this bacterium, yielding a partial genetic map. The strategy used here might be applicable to the construction of physical and genetic maps for other bacteria which have a relatively complex genomic architecture, and it might facilitate genomic mapping for organisms which are not amenable to conventional genetic-linkage mapping.

The existence of two chromosomes and the dispersal of



*rrn* cistrons between the linkage groups is but an additional indication of the versatility and complexity of the procaryotic gene pool. This complexity, with regard to both *R. sphaeroides* and the gene pool at large, warrants additional study.

#### ACKNOWLEDGMENTS

This work was supported by Public Health Service grant GM 31667 from the National Institutes of Health to S. Kaplan and by the Indonesian Second University Development Project (World Bank XVII) to A. Suwanto.

We thank P. L. Hallenbeck and R. A. Lerchen for all of the recombinant plasmids containing the CO<sub>2</sub> fixation gene(s) and  $\lambda$  rRNA, M. D. Moore for pUI551 and pUI553, S. C. Dryden for plasmids and fragment DNAs containing the *rrn* gene(s), J. K. Lee for pUI612, J. K. Wright for pRHBL19, W. A. Havelka for pUI710, and W. D. Shepherd for DNA fragments containing the *recA* gene. We also gratefully acknowledge C. Yun, J. Shapleigh, G. P. Roberts, J. F. Gardner, C. A. Gross, T. J. Donohue, J. D. Wall, R. V. Miller, and J. E. Walker for bacterial strains, bacteriophages, and plasmid DNA used in this study and Rudi Amann for the strain carrying the *tufB* recombinant plasmid. We also acknowledge the assistance of Sylvia C. Dryden for the interpretation of the *EcoRI* digest of the 214-kb *Asel* fragment in comparison with the *EcoRI* digestion of total genomic DNA.

#### LITERATURE CITED

- Allen, L. N., and R. S. Hanson. 1985. Construction of broad-host-range cosmid cloning vectors—identification of genes necessary for growth of *Methylobacterium organophilum* on methanol. *J. Bacteriol.* 161:955–962.
- Bachmann, B. J. 1983. Linkage map of *Escherichia coli* K-12, edition 7. *Microbiol. Rev.* 47:180–230.
- Banfalvi, Z., E. Kondorosi, and A. Kondorosi. 1985. *Rhizobium meliloti* carries two megaplasmids. *Plasmid* 13:129–138.
- Banfalvi, Z., V. Sakanyan, C. Koncz, A. Kiss, I. Dusha, and A. Kondorosi. 1981. Localization of nitrogen fixation genes on a high molecular weight plasmid of *Rhizobium meliloti*. *Mol. Gen. Genet.* 184:318–325.
- Bautsch, W. 1988. Rapid physical mapping of the *Mycoplasma mobile* genome by two-dimensional field inversion gel electrophoresis techniques. *Nucleic Acids Res.* 16:11461–11467.
- Bender, C. L., D. K. Malvick, and R. E. Mitchell. 1989. Plasmid-mediated production of the phytotoxin coronatine in *Pseudomonas syringae* pv. tomato. *J. Bacteriol.* 171:807–812.
- Birnboim, H. C., and J. Doly. 1979. A rapid alkaline extraction procedure for screening recombinant plasmid DNA. *Nucleic Acids Res.* 7:1513–1523.
- Bowien, B., M. Gusemann, R. Klintworth, and U. Windhovel. 1987. Metabolic and molecular regulation of the CO<sub>2</sub>-assimilating enzyme system in aerobic chemoautotrophs, p. 21–27. In H. W. Van Verseveld and J. A. Driine (ed.), *Microbial growth on C<sub>1</sub> compounds*. Martinus Nijhoff Publishers, Dordrecht, The Netherlands.
- Cohen-Bazire, G., W. R. Sistrom, and R. Y. Stanier. 1957. Kinetic studies of pigment synthesis by non-sulfur purple bacteria. *J. Cell. Comp. Physiol.* 49:25–68.
- Crofts, A. R., and C. A. Wraight. 1983. The electro-chemical domain of photosynthesis. *Biochim. Biophys. Acta* 726:149–185.
- Ely, B., and C. J. Gerardot. 1988. Use of pulsed-field gradient gel electrophoresis to construct a physical map of the *Caulobacter crescentus* genome. *Gene* 61:323–333.
- Frank, H. A., S. S. Taremi, and J. R. Knox. 1987. Crystallization and preliminary X-ray and optical spectroscopic characterization of the photochemical reaction center from *Rhodobacter sphaeroides* strain 2.4.1. *J. Mol. Biol.* 198:139–141.
- Frantz, B., and A. M. Chakrabarty. 1986. Degradative plasmids in *Pseudomonas*, p. 295–323. In J. R. Sokatch and L. N. Ornston (ed.), *The bacteria*, vol. 10. Academic Press, Inc., New York.
- Friedrich, B., C. G. Friedrich, M. Meyer, and H. G. Schlegel. 1984. Expression of hydrogenase in *Alcaligenes* spp. is altered by interspecific plasmid exchange. *J. Bacteriol.* 158:331–333.
- Friedrich, C. G., and B. Friedrich. 1983. Regulation of hydrogenase formation is temperature sensitive and plasmid coded in *Alcaligenes eutrophus*. *J. Bacteriol.* 153:176–181.
- Hallenbeck, P. L., and S. Kaplan. 1988. Structural gene regions of *Rhodobacter sphaeroides* involved in CO<sub>2</sub> fixation. *Photosynth. Res.* 19:63–71.
- Halloway, B. W. 1979. Plasmids that mobilize bacterial chromosome. *Plasmid* 2:1–19.
- Hightower, R. C., J. B. Bliska, N. R. Cozzarelli, and D. V. Santi. 1989. Analysis of amplified DNAs from drug-resistant *Leishmania* by orthogonal-field alteration gel electrophoresis: the effect of the size and topology on mobility. *J. Biol. Chem.* 264:2979–2984.
- Hogrefe, C., and B. Friedrich. 1984. Isolation and characterization of megaplasmid DNA from lithoautotrophic bacteria. *Plasmid* 12:161–169.
- Hogrefe, C., D. Römermann, and B. Friedrich. 1984. *Alcaligenes eutrophus* hydrogenase genes (Hox). *J. Bacteriol.* 158:43–48.
- Hynes, M. F., R. Simon, P. Müller, K. Niehaus, M. Labes, and A. Pühler. 1986. The two megaplasmids of *Rhizobium meliloti* are involved in the effective nodulation of alfalfa. *Mol. Gen. Genet.* 202:356–362.
- Hynes, M. F., R. Simon, and A. Pühler. 1985. The development of plasmid-free strains of *Agrobacterium tumefaciens* by using incompatibility with a *Rhizobium meliloti* plasmid to eliminate pATC58. *Plasmid* 13:99–105.
- Ingraham, J. L., M. Ole, and F. C. Neidhardt. 1983. Growth of the bacterial cell. Sinauer Associates, Inc., Publishers, Sunderland, Mass.
- Kahn, D., M. David, O. Domergue, M. Daveran, J. Ghai, P. R. Hirsch, and J. Batut. 1989. *Rhizobium meliloti* fixGHI sequence predicts involvement of a specific cation pump in symbiotic nitrogen fixation. *J. Bacteriol.* 171:929–939.
- Kaplan, S., and C. J. Arntzen. 1982. Photosynthetic membrane structure and function, p. 65–151. In Govindjee (ed.), *Photosynthesis: energy conversion by plants and bacteria*, vol. 1. Academic Press, Inc., New York.
- Kiley, P. J., and S. Kaplan. 1988. Molecular genetics of photosynthetic membrane biosynthesis in *Rhodobacter sphaeroides*. *Microbiol. Rev.* 52:50–69.
- Kinashi, H., and M. Shimaji. 1987. Detection of giant linear plasmids in antibiotic producing strains of *Streptomyces* by the OFAGE technique. *J. Antibiot.* 40:913–916.
- Kinashi, H., M. Shimaji, and A. Sakai. 1987. Giant linear plasmids in *Streptomyces* which code for antibiotic biosynthesis genes. *Nature (London)* 328:454–456.
- Klinworth, R., M. Husemann, J. Salmikow, and B. Bowien. 1985. Chromosomal and plasmid location for phosphoribulokinase genes in *Alcaligenes eutrophus*. *J. Bacteriol.* 164:954–956.
- Kohara, Y., K. Akiyama, and K. Isono. 1987. The physical map of the whole *Escherichia coli* chromosome. *Cell* 50:495–508.
- Komiyama, H., T. O. Yeates, D. C. Rees, J. P. Allen, and G. Feher. 1988. Structure of the reaction center from *Rhodobacter sphaeroides* R-26 and 2.4.1: symmetry relations and sequence comparisons between different species. *Proc. Natl. Acad. Sci. USA* 85:9012–9016.
- Kortlüke, C., C. Hogrefe, G. Eberz, A. Pühler, and B. Friedrich. 1987. Genes of lithoautotrophic metabolism are clustered on the megaplasmid pHG1 in *Alcaligenes eutrophus*. *Mol. Gen. Genet.* 210:122–128.
- Lee, J. J., H. O. Smith, and R. J. Redfield. 1989. Organization of the *Haemophilus influenzae* Rd genome. *J. Bacteriol.* 171:3016–3024.
- Lueking, D. R., R. T. Fraley, and S. Kaplan. 1978. Intracytoplasmic membrane synthesis in synchronous cell populations of *Rhodospseudomonas sphaeroides*. *J. Biol. Chem.* 253:451–457.
- McClelland, M., R. Jones, Y. Patel, and M. Nelson. 1987. Restriction endonucleases for pulsed field mapping of bacterial genomes. *Nucleic Acids Res.* 15:5985–6005.
- Piggot, P. J., and J. A. Hoch. 1985. Revised genetic linkage map

- of *Bacillus subtilis*. Microbiol. Rev. 49:158-179.
37. Poustka, A., and H. Lechrach. 1986. Jumping libraries and linking libraries: the next generation of molecular tools in mammalian genetics. Trends Genet. 7:174-179.
  38. Pyle, L. E., and L. R. Finch. 1988. A physical map of the genome of *Mycoplasma mycoides* subspecies *mycoides* Y with some functional loci. Nucleic Acids Res. 16:6027-6039.
  39. Sanderson, K. E., and J. R. Roth. 1988. Linkage map of *Salmonella typhimurium*, edition VII. Microbiol. Rev. 52:485-532.
  40. Sauer, K. 1986. Photosynthetic light reactions—physical aspects, p. 85-96. In L. A. Staehelin and C. J. Arntzen (ed.), Photosynthesis III: photosynthetic membranes. Encyclopedia of plant physiology, new series, vol. 19. Springer-Verlag, New York.
  41. Smith, C. L., J. G. Econome, A. Schutt, S. Kleo, and C. R. Cantor. 1987. A physical map of the *Escherichia coli* K12 genome. Science 236:1448-1453.
  42. Smith, C. L., P. E. Warburton, A. Gaal, and C. R. Cantor. 1986. Analysis of genome organization and rearrangements by pulsed field gradient gel electrophoresis, p. 45-70. In J. K. Setlow and A. Hollaender (ed.), Genetic engineering, vol. 8. Plenum Publishing Corp., New York.
  43. Suwanto, A., and S. Kaplan. 1989. Physical and genetic mapping of the *Rhodobacter sphaeroides* 2.4.1 genome: genome size, fragment identification, and gene localization. J. Bacteriol. 171:5840-5849.
  44. Tabata, S., A. Higashitani, M. Takanami, K. Akiyama, Y. Kohara, Y. Nishimura, A. Nishimura, S. Yasuda, and Y. Hirota. 1989. Construction of an ordered cosmid collection of the *Escherichia coli* K-12 W3110 chromosome. J. Bacteriol. 171:1214-1218.
  45. Tabita, F. R. 1988. Molecular and cellular regulation of autotrophic carbon dioxide fixation in microorganisms. Microbiol. Rev. 52:155-189.
  46. Van Larebeke, N., G. Engler, M. Holsters, S. Van den Elsacker, I. Zaenen, R. A. Schilperoort, and J. Schell. 1974. Large plasmid in *Agrobacterium tumefaciens* essential for crown gall-inducing ability. Nature (London) 242:171-172.